VOLUME 111, NUMBER 11
MAY 24, 1989
© Copyright 1989 by the American Chemical Society

JOURNAL
OF THE
AMERICAN
CHEMICAL
SOCIETY

Ab Initio Calculations of the Singlet–Triplet Energy Differences in Planar 2,4-Dimethylenecyclobutane-1,3-diyl and in Mono- and Dioxo Derivatives

Ping Du, David A. Hrovat, and Weston Thatcher Borden*

Contribution from the Department of Chemistry, University of Washington, Seattle, Washington 98195. Received August 31, 1988

Abstract: Ab initio calculations have been performed on the planar hydrocarbon diradical of the title (**1**) and on derivatives in which both (**2**) or one (**3**) of the exocyclic methylene groups are replaced by oxygen. The triplet is computed to be the ground state of planar **1**, but a singlet is unequivocally predicted to be the ground state of **2**. Although the average of the calculated singlet–triplet splittings in **1** and **2** might lead to the expectation of a singlet ground state for planar **3**, the triplet is actually computed to be lower in energy than the singlet. It is shown that this finding is largely due to additional electron delocalization in the triplet state of **3**, beyond the average of that in the triplet states of **1** and **2**. Correlation of the electrons in the σ orbitals with those in the π orbitals is found to be increasingly important for the accurate calculation of the singlet–triplet energy differences as the number of oxygen atoms increases. Differences between the electronic structures of these three diradicals, which are revealed in the optimized bond lengths and in the population analyses, are discussed.

2,4-Dimethylenecyclobutane-1,3-diyl (**1**) possesses a pair of π nonbonding MOs (NBMOs), which are shown schematically in Figure 1. Because these NBMOs have atoms in common, qualitative theory predicts a triplet ground state for **1**.[1] In fact, configuration interaction (CI) calculations, performed in the π space with the STO-3G basis set at the optimized geometries for the lowest singlet (^1A_g) and triplet ($^3B_{2u}$) state of planar **1**, found $^3B_{2u}$ to lie below ^1A_g by 23.6 kcal/mol.[2]

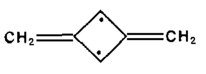

1

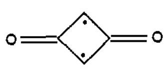

2

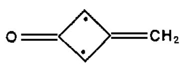

3

This is an upper limit to the adiabatic singlet–triplet gap, because the singlet prefers a nonplanar equilibrium geometry, which allows bonding between C-1 and C-3.[3,4] Nevertheless, the triplet is predicted to be at least metastable. Consistent with this prediction, triplet **1** has been generated by two different routes,[5,6] and the intensity of its EPR signal as a function of temperature has been found to give a linear Curie plot.

In contrast to the triplet ground state predicted for planar **1**, a semiempirical, PPP CI calculation indicated a singlet ground state for planar cyclobutane-2,4-dione-1,3-diyl (**2**).[7] Although the geometry of the ^1A_g state of planar **2** has been optimized with ab initio calculations,[4] ab initio calculations of the singlet–triplet energy separation in **2** have not been reported. In this paper we present the results of ab initio CI calculations of this energy difference in planar **2**.

---

[1] Davidson, E. R.; Borden, W. T. *J. Am. Chem. Soc.* **1977**, *99*, 4587. Borden, W. T. In *Diradicals*; Borden, W. T., Ed.; Wiley: New York, 1982; pp 1–72.

[2] Davidson, E. R.; Borden, W. T.; Smith, J. *J. Am. Chem. Soc.* **1978**, *100*, 3299.

[3] Feller, D.; Davidson, E. R.; Borden, W. T. *J. Am. Chem. Soc.* **1982**, *104*, 1216.

[4] Budzelaar, P. H. M.; Kraka, E.; Cremer, D.; Schleyer, P. v. R. *J. Am. Chem. Soc.* **1986**, *108*, 561.

[5] (a) Snyder, G. J.; Dougherty, D. A. *J. Am. Chem. Soc.* **1985**, *107*, 1774. (b) *Ibid.* **1986**, *108*, 299. (c) *Ibid.*, submitted for publication.

[6] Dowd, P.; Paik, Y. H. *J. Am. Chem. Soc.* **1986**, *108*, 2788.

[7] Gleiter, R.; Hoffmann, R. *Angew. Chem., Int. Ed. Engl.* **1969**, *8*, 214.

0002-7863/89/1511-3773$01.50/0 © 1989 American Chemical Society

Table I. π CI Optimized Geometry Parameters[a,b] of **1–3**

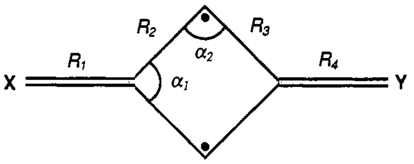

1, $X = Y = CH_2$

2, $X = Y = O$

3, $X = O, Y = CH_2$

molecule	state	R_1	R_2	R_3	R_4	α_1	α_2
1	$^3B_{2u}$	1.366	1.458	1.458	1.366	89.5	90.5
	^1A_g	1.337	1.486	1.486	1.337	87.2	92.8
2	$^3B_{2u}$	1.211	1.483	1.483	1.211	91.4	88.6
	^1A_g	1.198	1.480	1.480	1.198	87.6	92.4
3	$^3B_2$	1.201	1.492	1.439	1.389	88.6	89.3
	$^1A_1$	1.198	1.482	1.492	1.344	87.8	92.6

[a] Bond lengths in angstroms, bond angles in degrees. [b] See drawing for definitions of parameters.

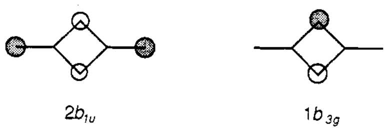

Figure 1. Schematic drawing of the NBMOs of **1**.

Although the ground state of diketone **2** has not been established experimentally, there is some experimental evidence of a triplet ground state for 4-methylenecyclobutan-2-one-1,3-diyl (**3**).[6] Dowd and Paik detected an EPR signal, whose intensity followed the Curie law and whose source they tentatively attributed to **3**. In this paper we also report the results of ab initio CI calculations of the energy difference between the lowest singlet and triplet state of planar **3**.

Computational Methodology

Preliminary geometry optimizations of the lowest triplet states of **1–3** were performed at the UHF level with the 6-31G* basis set.[8,9] Vibrational analyses showed the planar (D_{2h} for **1** and **2** and C_{2v} for **3**) geometry to be an energy minimum for the lowest triplet state of each of these diradicals. These calculations were carried out using the GAUSSIAN 82 package of ab initio programs.[10]

The geometries of the lowest singlet and triplet states of the planar diradicals were then reoptimized at the CI level. All CI calculations were carried out with an SVP basis set, consisting of the Dunning split-valence basis set, augmented with a set of polarization functions on the heavy atoms.[11] The CI calculations were performed with *K* orbitals,[12] which were generated from the RHF orbitals for the triplets and from the two-configuration (TC)SCF orbitals for the singlets. The MELD package[13] of ab initio programs was used for the CI calculations.

For the geometry reoptimizations, single-point CI calculations, which included all single and double π excitations from one reference configuration for the lowest triplet and from two configurations for the lowest singlet, were performed. These π-SD CI calculations involved 1037 and 1547 spin-adapted configurations, respectively, for the ^1A_g and $^3B_{2u}$ states of **1** and **2** and 2018 and 3085, respectively, for the $^1A_1$ and $^3A_2$ states of **3**.

The CI energies were fitted to quadratic potential energy functions in order to determine the optimal C–C and C–O bond lengths and the internal angles in the planar four-membered rings. The C–H bond lengths were frozen during these geometry optimizations, and each of the four bonds external to the ring was assumed to bisect the adjacent ring bond angle. The optimized geometries of **1–3** are given in Table I, and the RHF/TCSCF and π-SD CI energies are given in Table II.

Table II. Energies of the Lowest Singlet and Triplet States of **1–3** at Various Levels of Theory

molecule	calculation	E_S, hartree	E_T, hartree	ΔE,[a] kcal/mol
1	TCSCF/RHF[b]	−230.5678	−230.5783	6.6
	π-SD CI[c]	−230.6310	−230.6611	18.9
	MR-π-SD CI[d]	−230.6338	−230.6660	20.2
	MR-σ-S,π-SD CI[e]	−230.7556	−230.7847	18.2
2	TCSCF/RHF[b]	−302.3235	−302.2829	−25.5
	π-SD CI[c]	−302.3917	−302.3689	−14.3
	MR-π-SD CI[d]	−302.3942	−302.3736	−12.9
	MR-σ-S,π-SD CI[e]	−302.5533	−302.5202	−20.7
3	TCSCF/RHF[b]	−266.4422	−266.4431	0.5
	π-SD CI[c]	−266.5079	−266.5252	10.9
	MR-π-SD CI[d]	−266.5106	−266.5293	11.8
	MR-σ-S,π-SD CI[e]	−266.6512	−266.6635	7.7

[a] $\Delta E = E_S - E_T$, so a positive number indicates a triplet ground state. [b] Two-configuration SCF for the singlet and restricted Hartree-Fock for the triplet. [c] Singles and doubles CI in the π space. [d] Multireference singles and doubles CI in the π space. [e] Multireference CI, singles in the σ space plus singles and doubles in the π space.

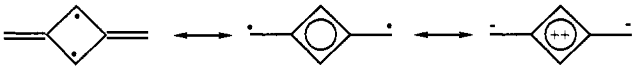

Figure 2. Possible resonance structures for **1**.

The effect on the relative energies of increasing the number of reference configurations was investigated by performing additional π CI calculations at the optimized π-SD CI geometries. All single and double π excitations were included from all the configurations formed by assigning the six π electrons to the six π orbitals of the conceptual minimal basis set. These multireference π CI calculations, which are designated MR-π-SD CI in Table II, involved 9698 and 14457 spin-adapted configurations, respectively, for the ^1A_g and $^3B_{2u}$ states of **1** and **2** and 19250 and 28897, respectively, for the $^1A_1$ and $^3B_2$ states of **3**.

In order to include correlation between the σ and π electrons, CI calculations were performed in which all single σ excitations from the six electron in six orbital π reference configurations were added to the single and double excited π configurations generated from the same reference list. For these calculations the six 1s core orbitals of the heavy atoms were frozen. We have previously found that this type of CI calculation, which includes all single π excitations from a multireference π wave function, gives a good account of σ–π correlation in radicals[14] and di-

---

(8) Hariharan, P. C.; Pople, J. A. *Theor. Chim. Acta* **1973**, *28*, 212.

(9) The optimized geometries and energies are available as supplementary material. Ordering information is given on any current masthead page.

(10) Binkley, J. S.; Frisch, M. J.; Raghavachari, M.; Fluder, E.; Seeger, R.; Pople, J. A., Carnegie-Mellon University.

(11) Dunning, T. H.; Hay, P. J. In *Methods of Electronic Structure Theory*; Schaefer, H. F., III, Ed.; Plenum: New York, 1977; Vol. 2.

(12) Feller, D.; Davidson, E. R. *J. Chem. Phys.* **1981**, *74*, 3977.

(13) Developed at the University of Washington by L. McMurchie, S. Elbert, S. Langhoff, and E. R. Davidson, and modified by D. Feller and D. Rawlings.

(14) Borden, W. T.; Davidson, E. R.; Feller, D. *J. Am. Chem. Soc.* **1981**, *103*, 5725. Hrovat, D. A.; Borden, W. T. *Ibid.* **1985**, *107*, 8034. Du, P.; Borden, W. T. *Ibid.* **1987**, *109*, 5330. Du, P.; Hrovat, D. A.; Borden, W. T. *Ibid.* **1988**, *110*, 3405.

Table III. Ratios of the Weights of the Two Most Important Configurations in the Wave Functions for the Lowest Singlet States of **1**-**3** at Various Levels of Theory

molecule	calculation[a]	c_1^2/c_2^2 [b]
1	TCSCF/RHF	2.96
	π-SD CI	2.71
	MR-π-SD CI	2.65
	MR-σ-S,π-SD CI	3.46
2	TCSCF/RHF	8.07
	π-SD CI	8.00
	MR-π-SD CI	7.97
	MR-σ-S,π-SD CI	12.59
3	TCSCF/RHF	4.52
	π-SD CI	4.29
	MR-π-SD CI	4.24
	MR-σ-S,π-SD CI	6.16

[a] See the footnotes to Table II for the meanings of the acronyms. [b] Where c_1 is the coefficient of $|...2b_{1u}^2\rangle$ ($|...2b_1^2\rangle$ in **3**), and c_2 is the coefficient of $|...1b_{3g}^2\rangle$ ($|...1a_2^2\rangle$ in **3**).

radicals[15] with charged π systems. These calculations are designated MR-σ-S,π-SD CI in Table II and included 75 390 and 120 413 spin-adapted configurations, respectively, for the ^1A_g and $^3B_{2u}$ states of **1**, 66 654 and 106 301 for the same two states of **2**, and 141 778 and 226 577, respectively, for the $^1A_1$ and $^3B_2$ states of **3**.

Results and Discussion

2,4-Dimethylenecyclobutane-1,3-diyl (1). The singlet and triplet π CI geometries of **1**, optimized with the SVP basis set, are similar to those obtained previously with the STO-3G basis set.[2] The bond lengths in Table I indicate that the ^1A_g wave function is more localized than that of $^3B_{2u}$, since the external double bonds are shorter and the ring bonds longer in ^1A_g than in $^3B_{2u}$. Resonance structures like the second in Figure 2 obviously contribute more to $^3B_{2u}$ than to ^1A_g.

As discussed elsewhere,[1,2] the greater localization of the π electrons in the singlet is a consequence of the fact that the two nonbonding electrons in this state have opposite spins. Hence, unlike the nonbonding electrons in the triplet, the pair in the singlet is not prohibited by the Pauli principle from appearing simultaneously in the same atomic orbital (AO). Localization of these two electrons in different regions of space, e.g. one at C-1 and the other at C-3, prevents these electrons from simultaneously occupying the same AO in the singlet and thus minimizes the Coulombic repulsion energy between them in this state.

In simple Hückel theory the two NBMOs of **1** are accidently degenerate in energy. However, the degeneracy does not survive a more rigorous theoretical treatment. For example, as shown in Table III, at all levels of theory the configuration $|...2b_{1u}\rangle$ has a substantially larger weight in the singlet wave function than the configuration $|...1b_{3g}\rangle$. Cross-ring bonding between C-1 and C-3, which is neglected in simple Hückel theory, is presumably a major contributor to favoring the occupancy of the $2b_{1u}$ MO.

Simple Hückel theory predicts that when the two NBMOs in **1** are equally occupied, the π-electron population on each carbon will be unity. Population analysis[16] of the $^3B_{2u}$ RHF wave function confirmed that this is essentially the case, as shown in Table IV. However, when, as in the ^1A_g TCSCF wave function, the $2b_{1u}$ NBMO has a substantially larger population than the $1b_{3g}$ NBMO, π-electron density is expected to be transferred from C-1 and C-3 to the two exocyclic carbons.[17] In fact, a population analysis of the ^1A_g wave function shows an excess of approximately 0.1 unit of π-electron density at each of the latter two carbons, whose source is largely the former two carbons. Thus, the third resonance structure in Figure 2 makes a significant contribution to the ^1A_g state of **1** but, of course, not to the $^3B_{2u}$ state.

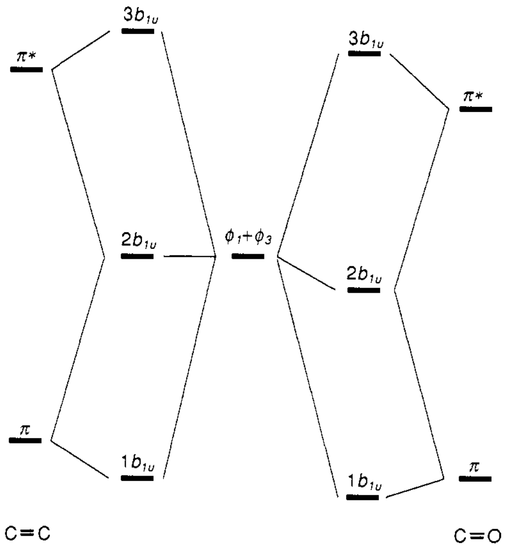

1 2

Figure 3. Schematic orbital interaction diagrams for the mixing in **1** and **3** of the b_{1u} combination of π AOs at C-1 and C-3 with the b_{1u} combinations of π and π^* orbitals of the exocyclic double bonds.

Because of the different contributions of the three resonance structures in Figure 2 to the lowest singlet and triplet state of **1**, inclusion of different types of electron correlation affects the energies of the two states differently. As shown in Table II, including correlation between all the π electrons selectively stabilizes $^3B_{2u}$, increasing the energy difference between it and ^1A_g from 6.6 kcal/mol at the RHF/TCSCF level to 18.9 kcal/mol at the π-SD CI level and to 20.2 kcal/mol at the MR-π-SD CI level of theory.

The triplet is selectively stabilized by π CI, because, as discussed above, the nonbonding electrons in this state are more delocalized than in the lowest singlet. Consequently, correlation between this pair of electrons and the four other π electrons is more important in the triplet than in the singlet. In contrast, inclusion of correlation between the σ and π electrons selectively stabilizes the more ionic π wave function of the singlet. Nevertheless, even with inclusion of σ–π correlation, the triplet is computed to lie 18.2 kcal/mol below the singlet in energy.

As shown in Table V, the calculated spin densities in the triplet are also affected by the inclusion of correlation between the π electrons. At the RHF level there is essentially no unpaired spin at C-2 and C-4, 0.74 unpaired π electron at C-1 and C-3, and 0.26 at each of the exocyclic carbons. This differs from the distribution of unpaired π electrons at these three sets of carbon atoms of, respectively, 0, 0.60, and 0.40 that is predicted by the simplest version of Hückel theory.

Inclusion of π-electron correlation increases the π spin densities at the two exocyclic carbons, C-5 and C-6, and introduces negative spin density at C-2 and C-4. When CI is performed, the ratio of π spin densities at C-1 and C-3 to those at C-5 and C-6 of about 1.6 is only slightly higher than the ratio of 1.5 predicted by simple Hückel theory.

The calculated π spin densities lead to the expectation that the hyperfine coupling constant for the hydrogens at C-1 and C-3 should be substantially larger than that for the hydrogens at C-5 and C-6. Experimentally, a seven-line pattern was observed for the $\Delta m = 2$ transition in the EPR spectrum of **1**.[5,6] Snyder and Dougherty interpreted this pattern as indicating similar hyperfine coupling constants for the two sets of nonequivalent hydrogens.[5a] Simulations of the spectrum gave a ratio of 1.2 ± 0.1 for the hyperfine coupling constants.[5c] However, the ratio of π spin densities obtained from our CI wave functions suggests a somewhat larger ratio of isotropic hyperfine coupling constants for the two

---

(15) Borden, W. T.; Davidson, E. R.; Feller, D. *J. Am. Chem. Soc.* **1980**, *102*, 5302. Review: Davidson, E. R.; Borden, W. T. *J. Chem. Phys.* **1983**, *87*, 4783.

(16) Populations were obtained by projecting the wave functions onto a minimal basis set of AOs, using the method of: Davidson, E. R. *J. Chem. Phys.* **1967**, *46*, 3319.

(17) When $2b_{1u}$ is doubly occupied, only the interaction betwen the π AOs at C-1 and C-3 and the π^* orbitals of the exocyclic double bonds results in electron transfer. Perturbation theory shows that the π-electron density that is transferred from C-1 and C-3 winds up on the two exocyclic atoms.

Table IV. Atomic π Orbital Population Analyses of the Lowest Singlet and Triplet States of **1**–**3** at Various Levels of Theory[a]

			population analyses				
molecule	state	calculation[b]	C_1 (C_3)	C_2	C_4	X	Y
1[c]	^1A_g	TCSCF	0.94	0.97	0.97	1.10	1.10
		π-SD CI	0.89	0.99	0.99	1.12	1.12
		MR-σ-S,π-SD CI	0.87	1.01	1.01	1.13	1.13
	$^3B_{2u}$	RHF	1.00	0.98	0.98	1.02	1.02
		π-SD CI	1.01	0.98	0.98	1.01	1.01
		MR-σ-S,π-SD CI	1.01	0.98	0.98	1.01	1.01
2[d]	^1A_g	TCSCF	0.87	0.69	0.69	1.40	1.40
		π-SD CI	0.77	0.80	0.80	1.39	1.39
		MR-σ-S,π-SD CI	0.75	0.83	0.83	1.37	1.37
	$^3B_{2u}$	RHF	0.93	0.74	0.74	1.30	1.30
		π-SD CI	0.94	0.81	0.81	1.23	1.23
		MR-σ-S,π-SD CI	0.94	0.82	0.82	1.21	1.21
3[e]	$^1A_1$	TCSCF	0.90	0.69	1.00	1.41	1.08
		π-SD CI	0.82	0.79	1.01	1.39	1.12
		MR-σ-S,π-SD CI	0.80	0.84	1.03	1.38	1.13
	$^3B_2$	RHF	1.02	0.70	0.94	1.39	0.91
		π-SD CI	1.00	0.77	0.95	1.31	0.94
		MR-σ-S,π-SD CI	1.00	0.79	0.95	1.29	0.95

[a] The MR-π-SD CI populations were essentially the same as those from the π-SD CI calculations, so only the latter are given in this table. [b] See the footnotes to Table II for the meanings of the acronyms. [c] X = Y = CH_2. [d] X = Y = O. [e] X = O, Y = CH_2.

Table V. Unpaired Electron Density in the π Atomic Orbitals of the Lowest Triplet States of **1**–**3** at Various Levels of Theory[a]

		population analyses				
molecule	calculation[b]	C_1 (C_3)	C_2	C_4	X	Y
1[c]	RHF	0.74	0.0	0.0	0.26	0.26
	π-SD CI	0.74	−0.19	−0.19	0.45	0.45
	MR-σ-S,π-SD CI	0.70	−0.16	−0.16	0.45	0.45
2[d]	RHF	0.85	0.02	0.02	0.13	0.13
	π-SD CI	0.84	−0.12	−0.12	0.28	0.28
	MR-σ-S,π-SD CI	0.79	−0.10	−0.10	0.30	0.30
3[e]	RHF	0.65	0.02	0.01	0.05	0.61
	π-SD CI	0.73	−0.06	−0.21	0.15	0.67
	MR-σ-S,π-SD CI	0.70	−0.05	−0.17	0.15	0.65

[a] The MR-π-SD CI densities were very similar to those from the π-SDCI calculations, so only the latter are given in this table. [b] See the footnotes to Table II for the meanings of the acronyms. [c] X = Y = CH_2. [d] X = Y = O. [e] X = O, Y = CH_2.

sets of nonequivalent hydrogens in **1**.[18]

Cyclobutane-2,4-dione-1,3-diyl (2). In the $^3B_{2u}$ state the greater length of the C–C bonds of the four-membered ring of **2**, compared to **1** (Table I), indicates that the carbonyl groups in **2** provide less electron delocalization than do the methylene groups in **1**. This conclusion is supported by comparison of the π spin densities in the triplet states of the two diradicals (Table V), which shows that more unpaired electron density is localized at C-1 and C-3 in **2** than in **1**. In contrast, in the ^1A_g state of **2** the ring bonds are actually slightly shorter than those in both the ^1A_g state of **1** and the $^3B_{2u}$ state of **2**. These differences between **1** and **2** can be understood on the basis of the orbital interaction diagrams shown in Figure 3.

In **1** the b_{1u} combination of π AOs at C-1 and C-3 mixes approximately equally with the b_{1u} combinations of both the bonding and antibonding π orbitals of the two exocyclic C–C double bonds. In **2** the lower energy of both the π and π^* orbitals of the two carbonyl groups and also the direction of polarization of these two orbitals, π toward oxygen and π^* toward carbon, causes the principal interaction of the π AOs at C-1 and C-3 to be with the latter orbital. This difference between **1** and **2** is illustrated in Figure 3 and has several important consequences.

First, because the nonbonding combination of AOs at C-1 and C-3 mixes strongly with two orbitals in **1** but largely with just a single orbital in **2**, one might anticipate that the resulting NBMO ($2b_{1u}$) would be more delocalized in **1** than in **2**. This was found to be the case on comparison of the RHF $2b_{1u}$ NBMOs for **1** and **2**. The greater localization of this NBMO to C-1 and C-3 in the $^3B_{2u}$ state of the latter diradical is responsible for the greater spin density at these two atoms in **2**.[19]

Second, because the bonding π orbitals of the exocyclic double bonds interact more strongly with the π AOs at C-1 and C-3 in **1** than in **2**, the coefficients at C-1 and C-3 in the lowest π MO ($1b_{1u}$) should be larger in **1** than in **2**. This was found to be true of the $1b_{1u}$ MOs from both the triplet RHF and singlet TCSCF calculations. Consequently, in both the lowest singlet and triplet states the $1b_{1u}$ MO provides more bonding between adjacent ring carbons in **1** than in **2**.

In the $2b_{1u}$ MO the mixing of the π AOs at C-1 and C-3 with the orbitals of the exocyclic double bonds occurs in an antibonding fashion for the π orbitals and in a bonding fashion for the π^* orbitals. Since the former interaction is weaker and the latter stronger in **2** than in **1**, the result is that the $2b_{1u}$ MO provides more bonding between adjacent ring carbons in **2** than in **1**.

In the $^3B_{2u}$ state of **1** and **2** only one electron occupies the $2b_{1u}$ MO. In this state the greater π bonding in **1** between the ring carbons in the doubly occupied $1b_{1u}$ MO is apparently sufficient to overcome the greater π bonding in **2** between these carbons in the singly occupied $2b_{1u}$ MO. This is presumably why the triplet state of **1** has a shorter ring bond length than the triplet state of **2**.

As the occupation number of the $2b_{1u}$ MO increases, the fact that this orbital is more bonding between the ring atoms in **2** than in **1** should tend to compensate more for the greater bonding between the ring carbons in the $1b_{1u}$ MO of **1**. This provides an explanation of the finding that, in contrast to the case in the $^3B_{2u}$ state, where the ring bonds of **2** are significantly longer than those in **1**, in the ^1A_g state the ring bonds of **2** are actually calculated to be slightly shorter than those of **1**.

The orbital interaction diagram in Figure 3 also predicts that mixing of the b_{1u} combination of AOs at C-1 and C-3 with the

---

[18] UHF calculations with the 6-31G* basis set give ratios of *atomic* spin densities at the ring and external carbons and at the hydrogens attached to them of, respectively, 1.26 and 0.91. Although these ratios appear to be in better agreement with experiment than those obtained from our CI calculations, it should be noted that the value of S^2 for the UHF wave function of triplet **1** is 2.48, which indicates significant contamination of the triplet wave function by higher multiplicities. In contrast, our CI wave functions are pure triplets; and we believe that the spin densities obtained from them are, therefore, more likely to be quantitatively correct. Inclusion of excitations through quadruples in the π CI wave function (π-SDTQCI) gives essentially the same spin densities as π-SD CI.

[19] Since essentially the same orbital interaction diagrams as those in Figure 3 would be constructed to compare allyl with $H_2C{-}CH{=}O$, one would expect much less delocalization of the unpaired electron in the latter radical than in the former. This qualitative expectation is in agreement with the quantitative results of ab initio calculations (Huyser, E. S.; Feller, D.; Borden, W. T.; Davidson, E. R. *J. Am. Chem. Soc.* **1982**, *104*, 2956) and with the spin densities observed in radicals that are α to carbonyl groups (Camaioni, D. M.; Walter, H. F.; Jordan, J. E.; Pratt, D. W. *J. Am. Chem. Soc.* **1973**, *95*, 7978).

π and π^* orbitals of the two exocyclic double bonds will result in a larger stabilization of the resulting $2b_{1u}$ MO in **2** than in **1**. Since the b_{3g} combination of AOs at C-1 and C-3 does not mix with the orbitals of the exocyclic double bonds, it follows that the energy difference between $2b_{1u}$ and $1b_{3g}$ will be substantially larger in **2** than in **1**.[20] This expectation is confirmed by comparing the weights of $|...2b_{1u}{}^2\rangle$ and $|...1b_{3g}{}^2\rangle$ in the wave functions for the ^1A_g states of **1** and **2**. As shown in Table III, at all levels of theory the ratio of the square of the coefficient of the former configuration to that of the latter is much larger in **2** than in **1**.

Because the $2b_{1u}$ and $1b_{3g}$ MOs are each occupied by one electron in the $^3B_{2u}$ state, whereas the occupancy of the former orbital can approach two in the ^1A_g state (and does so in **2**), the ^1A_g state should be significantly stabilized, relative to $^3B_{2u}$, on going from **1** to **2**.[21] In fact, as shown in Table II, on going from **1** to **2**, the ^1A_g state is computed to be stabilized, relative to $^3B_{2u}$, by 32–39 kcal/mol. Thus, in contrast to the triplet ground state computed for planar **1**, the ground state of **2** is unequivocally predicted to be a singlet.

In both the singlet and triplet states of **2**, there is, as shown by the population analyses in Table IV, some transfer of π electron density from C-1 and C-3 into the two carbonyl groups. This is explicable, since as illustrated in Figure 3, the π AOs at C-1 and C-3 interact principally with the π^* orbitals of the carbonyl groups, which are empty. Moreover, on going from the triplet to the singlet state of **2**, a substantial amount of π-electron density is transferred from the $1b_{3g}$ MO, which is confined by symmetry to C-1 and C-3,[22] to the $2b_{1u}$ MO, which has appreciable density on the two oxygens. This accounts for the greater transfer of π-electron density from C-1 and C-3 to the two oxygens in the singlet than in the triplet.

In both **1** and **2** the greater ionic character of the π wave function for singlet, compared to that for the triplet state, results in selective stabilization of the singlet on inclusion of σ–π correlation. However, because the difference between the ionic character of the π wave functions for these two states is larger in **2** than in **1** (Table IV), inclusion of σ–π correlation results in a roughly 4 times greater selective stabilization of the singlet state in **2** than in **1** (Table II).

4-Methylenecyclobutan-2-one-1,3-diyl (3). Although it might have been expected that the properties of **3** would be the average of those of **1** and **2**, our computational results reveal that this is not the case. The bond lengths in the $^3B_2$ state of **3** indicate that the lone C–C π bond provides more electron delocalization than either of the C–C π bonds in triplet **1** and that the carbonyl group of **3** provides less electron delocalization than either of the individual carbonyl groups in triplet **2**. This conclusion is supported by the unpaired electron densities in Table V. At all levels of theory the spin density at the exocyclic methylene carbon of **3** is very much larger than that at either of the corresponding carbons in **1**, and the spin density at the oxygen in **3** is smaller than that at either oxygen of **2**. The spin density at the exocyclic methylene group in **3** is, in fact, nearly as large as that at C-1 and C-3.

From Figure 3 and the accompanying discussion of the differences between **1** and **2**, it is clear that a vinylidene group provides more delocalization than does a carbonyl group when a single electron occupies the b_1 combination of AOs at C-1 and C-3. Thus, when one of the exocyclic methylene groups in **1** is replaced by an oxygen, the smaller amount of delocalization provided by the carbonyl group in the triplet state of the resulting diradical (**3**) allows the remaining vinylidene group to provide more electron delocalization than does either of the individual vinylidene groups in **1**. Similarly, replacing an oxygen in **2** by a methylene demands less electron delocalization of the remaining carbonyl group in triplet **3** than is required of either of the carbonyl groups in **2**.

Because of the strong interaction involving the vinylidene group in the triplet state of **3**, the electronic structure of this state of **3** is better viewed as being that of a triplet trimethylenemethane (TMM) interacting weakly with a carbonyl group rather than as the average of the electronic structures of triplet **1** and **2**. The near equality of the spin density at the exocyclic methylene group with that at C-1 and C-3 in triplet **3** lends support to this model.

The additional electron delocalization, beyond the average of that in **1** and **2**, that is present in the triplet state of **3** should have the consequence that the energy of triplet **3** should be lower than the average of the energies of triplet **1** and **2**. In fact, the reaction

$$\tfrac{1}{2}\mathbf{1} + \tfrac{1}{2}\mathbf{2} \rightarrow \mathbf{3} \qquad (1)$$

is calculated from the triplet energies in Table II to be exothermic by 7.2 kcal/mol at the RHF, 6.4 kcal/mol at the π-SD CI, 6.0 kcal/mol at the MR-π-SD CI, and 6.9 kcal/mol at the MR-σ-S,π-SD CI level of theory.

As discussed above, in the singlet state of **1** minimization of the Coulombic repulsion energy between the nonbonding electrons results in much less electron delocalization than in the triplet state. Consequently, replacement of an exocyclic methylene group in **1** by an oxygen would be expected to effect a much smaller change in the amount of electron delocalization by the remaining vinylidene group in the singlet state of **3** than in the triplet state.

In fact, as shown in Table I, in the singlet state of **3** the lengths of the bonds to and in the exocyclic vinylidene group are quite close to those in **1**. Moreover, in the singlet state of **3** the lengths of the bonds to and in the carbonyl group are essentially the same as those in **2**. Thus, unlike the case in the triplet state of **3**, the bonding in the singlet appears to be approximately the same as that in the relevant portions of singlet **1** and **2**. This conclusion is supported by comparison of the population anlaysis in Table IV for the singlet state of **3** with those for the singlet states of **1** and **2**.

If the combination of vinylidene and carbonyl groups provides no special stabilization for singlet **3**, the reaction in eq 1 should be approximately thermoneutral. From the singlet energies in Table II, this reaction is actually computed to be *endothermic* by about 2 kcal/mol at all levels of theory. This finding provides additional evidence that, in contrast to the case in the triplet state of **3**, in the singlet state the stabilization of the radical centers at C-1 and C-3 by the vinylidene and carbonyl groups is nonsynergistic.[23]

As shown in Table II, the triplet is predicted to be the ground state of **3** at all levels of theory. As is the case with **1** and **2**, the size of the singlet–triplet splitting depends on the type of electron correlation that is included. However, at each level of theory the triplet state of **3** lies below the singlet by an amount that ranges from 8 to 9 kcal/mol more than the average of the singlet–triplet separations in **1** and **2**. As discussed above, roughly three-quarters of this difference between the singlet–triplet splitting in **3** and the average of those in **1** and **2** is due to the lower than average energy of the triplet state of **3** and about one-quarter to the greater than average energy of the singlet.

The results of our calculations on planar **3** predict that it should have a triplet ground state. Therefore, our computational results certainly allow the possibility that the EPR signal, observed by

---

[20] The same argument can be made by applying first-order perturbation theory to the NBMOs of **1**. However, since first-order perturbation theory does not include the changes in the MOs on going from **1** to **2**, many of the other differences between these two diradicals are not predicted by this type of analysis.

[21] Because of the parallel between the orbital interaction diagrams in Figure 3 and those for allyl and H_2C—CH═O, the same line of reasoning allows one to understand the differences between the stabilization provided by C–C and C–O π bonds adjacent to radical and carbanion centers. Although an adjacent C–C π bond provides slightly more stabilization for a radical than does an adjacent C–O π bond (Pasto, D. J.; Krasnansky, R. Zercher, C. *J. Org. Chem.* **1987**, *52*, 3062 and references therein), a C–O π bond has a much larger effect than a C–C π bond on stabilizing an adjacent carbanion and thus increasing the gas-phase acidity of an α C–H bond (Bartmess, J. E.; McIver, R. T., Jr. In *Gas Phase Ion Chemistry*; Bowers, M. T., Jr., Ed.; Academic Press: New York, 1979; pp 87–121).

[22] This is only strictly true with an unpolarized basis set, since suitable combinations of d_{yz} orbitals at C-2 and C-4 and on the exocyclic atoms also have b_{3g} symmetry.

[23] The calculated endothermicity of the reaction in eq 1 for the singlet states may be due to synergism between the two oxygens in **2** in favoring occupancy of the $2b_{1u}$ NBMO.

3778 *J. Am. Chem. Soc.* **1989**, *111*, 3778-3782

Dowd and Paik and assigned to triplet **3**,[6] actually does belong to this diradical.

Acknowledgment. We thank the National Science Foundation for support of this research. The purchase of the Convex C-1 computer, which was used for some of the calculations, was also made possible by a grant from NSF. Several of the calculations reported here were performed at the San Diego Supercomputer Center, which we thank for a generous grant of supercomputer time.

Supplementary Material Available: UHF 6-31G* geometries and energies of the lowest triplet state of **1**–**3** (3 pages). Ordering information is given on any current masthead page.

Origin of Metal Clustering in Transition-Metal Chalcogenide Layers MX_2 (M = Nb, Ta, Mo, Re; X = S, Se)

Enric Canadell,*,[1a] Albert LeBeuze,*,[1b] Moulay Abdelaziz El Khalifa,[1b] Roger Chevrel,[1c] and Myung-Hwan Whangbo*,[1d]

Contribution from the Laboratoire de Chimie Théorique,[†] Bât. 490, Université de Paris-Sud, 91405 Orsay, France, Laboratoire de Chimie Théorique, Université de Rennes I, 35042 Rennes, France, Laboratoire de Chimie Minérale B, Université de Rennes I, 35402 Rennes, France, and Department of Chemistry, North Carolina State University, Raleigh, North Carolina 27695-8204. *Received September 15, 1988*

Abstract: The origin of metal clustering in transition-metal layers MX_2 (M = transition metal, X = chalcogen) was examined by performing tight-binding band electronic structure calculations on $CoMo_2S_4$, V_3S_4, Mo_2S_3, and Nb_2Se_3. Since all MX_2 layers that exhibit metal clustering have double octahedral M_2X_6 chains as their building blocks, we analyzed the metal clustering in the MX_2 layers as a phenomenon concerning its building blocks, M_2X_6 chains. Our study shows that the metal clustering in an MX_2 layer of d^2 ions arises from the metal–metal bond formation across shared octahedral edges between MX_4 chains of each M_2X_6 chain. The metal clustering in an MX_2 layer of d^3 ions is a consequence of the Peierls distortion associated with the half-filled t_{2g} block bands of its building blocks, M_2X_6 chains.

Metal clustering is often observed in MX_2 layers made up of MX_6 octahedra (M = transition metal, X = halogen).[2-7] It is appealing to analyze the origin of the metal clustering from the viewpoint of the electronic structure change associated with a distortion from an ideal, hexagonal MX_2 layer.[8] However, this analysis is complicated due to the absence of simple distortion parameters connecting the ideal structure to the real one. All MX_2 layers that show metal clustering have M_2X_6 chains as their building blocks (vide infra), so it would be simple to describe the metal clustering as a phenomenon concerning the M_2X_6 chains rather than the MX_2 layers. This alternative approach provides a much simpler description for the crystal and electronic structures of numerous transition-metal chalcogenides containing MX_2 layers, which include ReX_2 (X = S, Se),[2] $M'Mo_2S_4$ (M′ = V, Cr, Fe, Co),[3] NiV_2X_4 (X = S, Se),[4] V_3X_4 (X = S, Se),[5] Mo_2S_3,[6] and M_2Se_3 (M = Nb, Ta).[7] In the present work, we discuss the electronic structures of these compounds from the viewpoint of their building blocks, M_2X_6 chains. In the following, the structural patterns of those compounds are briefly reviewed, and the origin of their metal clustering is discussed in terms of the tight-binding band electronic structures calculated for several representative examples.

M_2X_6 Chains as Building Blocks

An ideal MX_4 chain **1** is obtained from regular MX_6 octahedra upon edge sharing. Similarly, an ideal M_2X_6 chain **2** is obtained from two ideal MX_4 chains via edge sharing. By repeating this process, one obtains an ideal MX_2 layer **3**. For our discussion, it is important to note that the layer **3** is also derived from the M_2X_6 chains **2** upon edge sharing. A projection view of **3** perpendicular to the layer is given by **4a**, which shows only the metal atoms and the upper triangle of X atoms around each metal. Ideal M_2X_6 chains have no metal–metal bonding as schematically

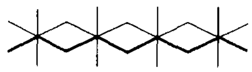

1

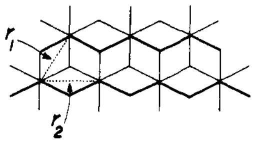

2

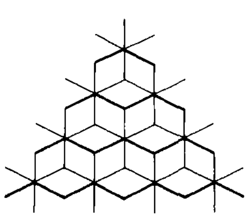

3

[†] The Laboratoire de Chimie Théorique is associated with the CNRS (UA 506) and belongs to ICMO and IPCM (Orsay).

(1) (a) Université de Paris-Sud. (b) Laboratoire de Chimie Théorique, Université de Rennes I. (c) Laboratoire de Chimie Minérale B, Université de Rennes I. (d) North Carolina State University.

(2) (a) Alcock, N. W.; Kjekshus, A. *Acta Chem. Scand.* **1965**, *19*, 79. (b) Wildervanck, J. C.; Jellinek, F. *J. Less-Common Met.* **1971**, *24*, 73.

(3) (a) van de Berg, J. M. *Inorg. Chim. Acta* **1968**, *2*, 216. (b) Anzenhofer, K.; de Boer, J. J. *Acta Crystallogr.* **1969**, *B25*, 1419. (c) Guillevic, J.; Le Marouille, J.-Y.; Grandjean, D. *Acta Crystallogr.* **1974**, *B30*, 111. (d) Chevrel, R.; Sergent, M.; Meury, J. L.; Quan, D. T.; Colin, Y. *J. Solid State Chem.* **1974**, *10*, 260. (e) Chevrel, R. Thèse d'Etat, Université de Rennes, 1974, pp 22–73. (f) Wada, H.; Onoda, M.; Nozaki, H.; Kawada, I. *J. Solid State Chem.* **1986**, *63*, 369.

0002-7863/89/1511-3778$01.50/0 © 1989 American Chemical Society